Bull. Soc. géol. France, 2012, t. 183, n° 4, pp. 369-382

Bajocian to Tithonian age of radiolarian cherts in the Tolmin basin (NW Slovenia)

Špela GORIČAN[1], Jernej PAVŠIČ[2] and Boštjan ROŽIČ[2]

Key words. – Tolmin basin, Southern Alps, Dinarides, Jurassic, Chert, Radiolaria, Nannoplankton.

Abstract. – The Tolmin basin is a typical example of a deep-water Mesozoic basin that developed on the rifted south Tethyan continental margin. Remnants of this basin are preserved at the intersection of the Dinarides and the southern Alps in northwestern Slovenia. The Jurassic successions consist of carbonate gravity-flow deposits, radiolarian cherts and shales, and are overlain by pelagic Biancone limestone. A distinctive chert-dominated interval (the upper member of the Tolmin Formation) was dated with radiolarians. The base of this interval was assigned to the late Bajocian in the distal part of the basin and to the middle Callovian-early Oxfordian in the more proximal part of the basin. The topmost radiolarian cherts are early Tithonian in age. The mid-Tithonian transition from chert to the Biancone limestone was also determined with nannoplankton. The beginning of highly siliceous sedimentation in the Bajocian correlates well over the entire western Tethys and was linked to two factors: an increase in water depth due to regional subsidence and an increase in plankton productivity. The pronounced silica enrichment coincided with the opening of the Alpine Tethys and with the intraoceanic subduction that occurred in the Meliata-Maliac-Vardar Ocean. Reorganization of the plate boundaries may have induced substantial changes in the circulation of water masses that, in turn, had a long-term effect on surface productivity. On the basin scale, radiolarian dating revealed considerable lateral and vertical variations in the thickness of chert successions. This distributional pattern implies that, in narrow continental-margin basins, sedimentation rates were primarily determined by the redeposition of pelagic sediments. Important stratigraphic gaps occur even in the distal basinal setting.

L'âge bajocien à tithonien des cherts à radiolaires dans le bassin de Tolmin (nord-ouest de la Slovénie)

Mots-clés. – Bassin de Tolmin, Alpes du Sud, Dinarides, Jurassique, Chert, Radiolaires, Nannoplancton.

Résumé. – Le bassin de Tolmin est un exemple typique de bassin mesozoïque relativement profond qui s'est formé pendant le rifting de la marge continentale sud-téthysienne. Les dépôts sédimentaires de ce bassin sont préservés à l'intersection entre les Dinarides et les Alpes du Sud en Slovénie nord-occidentale. Les séries jurassiques sont composées de carbonates resédimentés, de cherts à radiolaires et d'argiles et elle sont surmontées par le calcaire pélagique de Biancone. Un intervalle distinct, dominé par les cherts (le membre supérieur de la formation de Tolmin), a été daté avec des radiolaires. La base de cet intervalle a été attribuée au Bajocien supérieur dans la partie distale du bassin et au Callovien moyen-Oxfordien inférieur dans la partie plus proximale du bassin. Le sommet des cherts à radiolaires est d'âge tithonien inférieur. La transition des cherts au calcaire de Biancone au Tithonien moyen a été également datée grâce au nannoplancton. Le début de la sédimentation fortement siliceuse au Bajocien était à peu près synchrone dans l'ensemble des bassins de la Téthys occidentale et il était lié à deux facteurs : l'augmentation de la profondeur d'eau suite à une subsidence régionale et l'augmentation de la productivité du plancton. L'enrichissement marqué en silice a coïncidé avec l'ouverture de la Téthys Alpine et avec la subduction intraocéanique dans l'océan de Meliata-Maliac-Vardar. La réorganisation des limites des plaques lithosphériques a pu conduire aux changements majeurs de la circulation des masses d'eau, ce qui par la suite a eu un effet à long terme sur la productivité en surface. A l'échelle du bassin, les datations à radiolaires révélent des variations latérales et verticales considérables de l'épaisseur des séries à chert. Cette répartition implique que dans les bassins étroits des marges continentales, les taux de sédimentation étaient principalement déterminés par la redistribution des sédiments pélagiques. Des lacunes stratigraphiques importantes existent même dans les parties distales du bassin.

INTRODUCTION

Radiolarians are the most important and often the only fossils available to date siliceous deep-sea deposits. Over the last three decades, extensive radiolarian studies have been undertaken in stratigraphic research on Mesozoic pelagic rocks in the Mediterranean region. However, radiolarian cherts of several Jurassic basins still lack the stratigraphic precision required for accurate regional correlations.

The study area is located in the eastern part of the southern Alps (fig. 1a) where the South Alpine and the Dinaric

1. Ivan Rakovec Institute of Paleontology, ZRC SAZU, Novi trg 2, SI-1000 Ljubljana, Slovenia. spela@zrc-sazu.si
2. Department of Geology, Faculty of Natural Sciences and Engineering, University of Ljubljana, Privoz 11, SI-1000 Ljubljana, Slovenia.
Manuscript deposited on May 15, 2011; accepted on February 17, 2012.

structures now overlap. In the Mesozoic and early Tertiary, this area clearly evolved as part of the NW-SE oriented Dinaric system [Placer, 1999]. Only later, in the Neogene, were the Dinaric structures overprinted by southward-directed Alpine thrusting [Doglioni and Bosellini, 1987; Doglioni and Siorpaes, 1990; Placer, 1999]. The nappe system in the research area derived from the continental margin of the Adriatic microplate. In the Middle and Late Jurassic, this part of the margin was facing the Meliata-Maliac remnant basin and the Vardar Ocean, which together formed a single branch of the Neotethys [Schmid *et al.*, 2008], but was also close to the Alpine Tethys (see fig. 1b).

During the latest Triassic and Early Jurassic, the continental margin experienced a major period of extensional tectonics related to the reorganization of lithospheric plates due to the breakup of Pangea and the formation of the Atlantic Ocean. An array of grabens and horsts was created by episodic differential subsidence [Bernoulli *et al.*, 1990; Sarti *et al.*, 1992; Bertotti *et al.*, 1993; Berra *et al.*, 2009]. The extent of this rifting was regional and has been well documented from the western Mediterranean to the Arabian Peninsula [Schettino and Turco, 2011]. During the Middle to Late Jurassic, after the final opening of the Alpine Tethys, the region became progressively deeper due to post-rift thermal subsidence. From the Bajocian onwards, the elevated areas were submerged submarine plateaus with condensed pelagic sedimentation and considerable stratigraphic gaps. The surrounding basins subsided to bathyal depths and were mostly characterized by highly siliceous pelagic sediments, occasionally punctuated by calcareous turbidites from adjacent platforms.

The following paleotopographic units have been distinguished in NW Slovenia (for the present-day facies distribution, see fig. 1a): the Bovec basin, which formed near the end of the Early Jurassic, the Julian high (comparable to the Trento plateau of the southern Alps) and the Bled and Tolmin basins that existed from the Triassic [Cousin, 1981; Buser, 1986, 1996; Šmuc, 2005; Rožič, 2009; also see Kukoč *et al.*, 2012]. The large stable Dinaric Carbonate Platform (also named the Friuli Carbonate Platform or the Adriatic Carbonate Platform) further south persisted throughout the Jurassic and continued to grow in the Cretaceous. The Jurassic stratigraphy of individual units is generally well known but precise age constraints are still missing for many pelagic sequences.

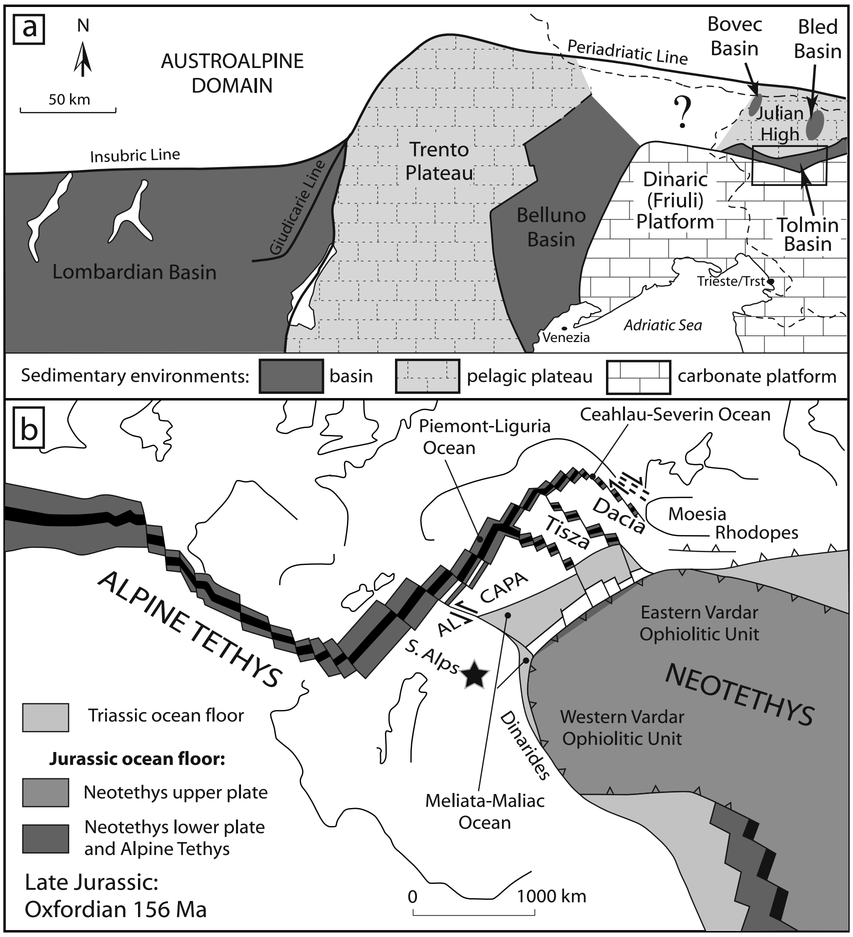

FIG. 1a. – Present-day position of paleogeographic units [according to Winterer and Bosellini, 1981; Šmuc and Goričan, 2005]. The area in the rectangle is enlarged in figure 2a.
FIG. 1b. – Paleogeographic reconstruction for the Oxfordian [after Schmid *et al.*, 2008] with the location of the Tolmin basin marked (star symbol).
FIG. 1a. – *Position actuelle des unités paléogéographiques [d'après Winterer et Bosellini, 1981; Šmuc et Goričan, 2005]. La région encadrée est agrandie dans la figure 2a.*
FIG. 1b. – *Reconstruction paléogéographique à l'Oxfordien [d'après Schmid* et al.*, 2008] avec la localisation du bassin de Tolmin (symbole étoile).*

In highly siliceous pelagic rocks such as cherts, mudstones and siliceous limestones, radiolarians are often the only guide fossils and are thus indispensable for deciphering the evolution of deep-water sedimentary basins. Ever since the early development of the Middle and Upper Jurassic radiolarian time scales approximately 30 years ago [Baumgartner *et al.*, 1980; Kocher, 1981; Baumgartner, 1984], radiolarian dating has been used as a basic biostratigraphic method to reconstruct the rifting histories of continental margins. Bedded cherts of the Lombardian basin and the Trento plateau in the southern Alps were among the first pelagic deposits studied in terms of radiolarians [Kocher, 1981; Baumgartner, 1984]. In this example, it was clearly demonstrated how profoundly the supposed contemporaneousness of the siliceous facies found across different parts of the margin [Winterer and Bosellini, 1981] had to be modified when radiolarian age constraints became available [see Figures. 3 and 4 in Baumgartner *et al.*, 1995b]. Further studies on additional sections in the southern Alps, including the Belluno Basin, produced a wealth of new data that now allow a more detailed reconstruction of the complex horst and graben topography in this part of the Adriatic continental margin [Baumgartner *et al.*, 1995b; Beccaro *et al.*, 2002; Beccaro, 2006a, 2006b; Chiari *et al.*, 2007; Beccaro *et al.*, 2008]. Several other Jurassic basinal successions of the Adriatic margin, e.g., in the Apennines [De Wever and Miconnet, 1985; Baumgartner, 1990; Bartolini *et al.*, 1995, 1996, 1999] and in the Dinarides-Hellenides [Danelian *et al.*, 1986; De Wever and Cordey, 1986; Danelian and Baudin, 1990; Goričan, 1994; Danelian *et al*., 1997; Djerić *et al.*, 2007; Vishnevskaya and Djerić, 2009], have also been satisfactorily dated with radiolarians. In NW Slovenia, systematic radiolarian dating has only recently been introduced in stratigraphic research of deep-water Jurassic successions. Middle and Late Jurassic radiolarian ages have so far only been published for one basinal succession, located at Mt. Mangart [Šmuc and Goričan, 2005] and paleogeographically ascribed to the Bovec basin [Cousin 1981; Šmuc, 2005].

The present contribution focuses on the Tolmin basin, which was first studied in the 1970s and 1980s [Cousin, 1970, 1973, 1981; Buser, 1986, 1987] and has since been restudied in more detail in the last few years [Rožič, 2006, Rožič and Popit, 2006; Rožič, 2009]. Rožič [2009] formally described the Middle and Upper Jurassic basinal deposits as the Tolmin Formation. Based on preliminary radiolarian results [Goričan *et al.*, 2006], he assigned a Bajocian to Early Tithonian age to the upper, chert-dominated member of the Tolmin Formation; however, no radiolarian data have been documented and discussed adequately yet. The aim of this paper is to present radiolarian assemblages that allow age assignments and to discuss the distribution of radiolarian cherts at the local (intrabasinal) and regional scales.

GEOLOGICAL SETTING

Two composite south-verging tectonic units, namely, the Tolmin nappe and the Julian nappe, which overthrusts the Tolmin nappe, are generally distinguished in the southern Alps of NW Slovenia [Placer, 1999] (see fig. 1a for their geographic location). To the north, the southern Alps are separated from the Austroalpine units by the Periadriatic Line; to the south, the southern Alpine front is in direct contact with the Trnovo nappe of the External Dinarides [Placer, 1999]. In terms of the aforementioned paleogeographic units (fig. 1a), the Trnovo nappe and the Tolmin nappe (fig. 2a) correspond to the Dinaric Carbonate Platform and the Tolmin basin, respectively. The Julian nappe is tectonically more complex and comprises stratigraphic successions of the Bovec and Bled basins as well as those of the Julian High (fig. 1a).

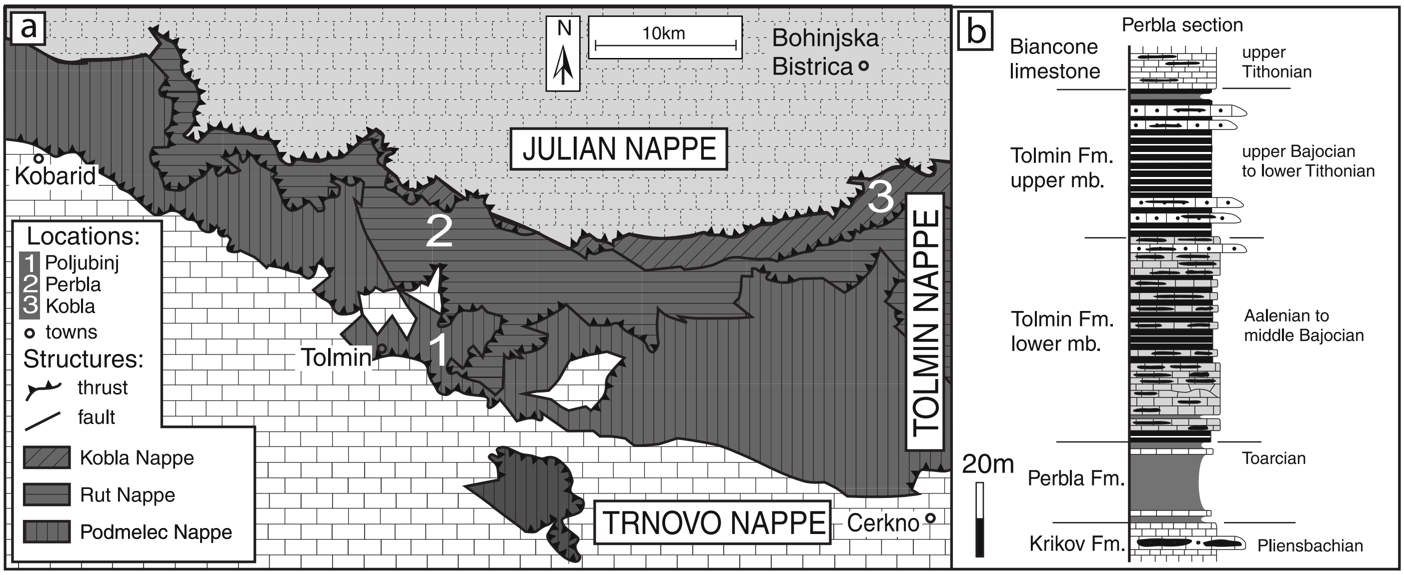

FIG. 2a. – Structural map of the investigated area with the locations of the three studied sections.
FIG. 2a. – General stratigraphy of the Tolmin basin, as observed in the Perbla section (type section of Perbla and Tolmin formations). Both figures are from Rožič [2009]. The legend for the lithologies is the same as for figure 3.
FIG. 2a. – *Carte structurale de la région d'étude avec la localisation des trois coupes étudiées.*
FIG. 2b. – *Stratigraphie générale du bassin de Tolmin observée sur la coupe de Perbla (localité type des formations de Perbla et de Tolmin). Les deux figures sont de Rožič [2009]. La légende pour les lithologies est la même que dans la figure 3.*

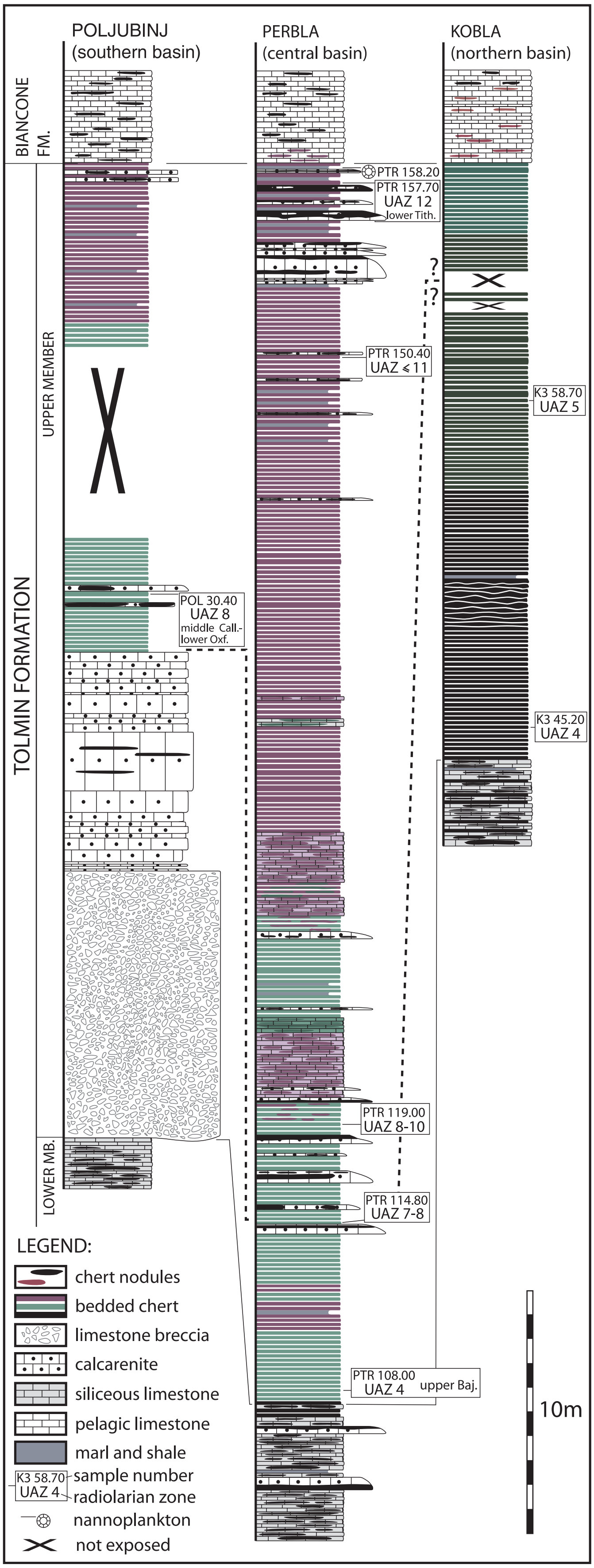

FIG. 3. – Detailed stratigraphic logs, including the positions of the radiolarian and nannoplankton samples.
FIG. 3. – *Colonnes stratigraphiques détaillées et position des échantillons à radiolaires et à nannoplancton.*

The Tolmin nappe (fig. 2a) is generally subdivided into three second-order nappes. From bottom to top these are the Podmelec nappe, the Rut nappe and the Kobla nappe [Buser, 1986, 1987]. The Ponikve klippe (fig. 2a) lies further south on top of the Trnovo nappe [Buser, 1987; Placer, 1999]. In terms of paleogeography, the stratigraphic successions of these nappes correspond to different parts of the Tolmin basin. Different proximal to distal successions are now juxtaposed primarily because of the Neogene N-S shortening. Facies variations in the W-E direction have also been observed; these variations reflect the original NW-SE basin orientation, which was amplified by older, i.e., Paleogene, thrusting towards the southwest [Rožič, 2009]. The Triassic to Cretaceous rocks of the Tolmin nappe exhibit a considerable thermal overprint, which occurred in post-Late Cretaceous to pre-Mid Oligocene times [Rainer *et al.*, 2009]. Vitrinite reflectance and illite crystallinity studies have demonstrated that these rocks were subject to deep diagenesis and, in the area NE of Cerkno (see fig. 2a), reached the anchizone [Rainer *et al.*, 2002, 2009].

The Jurassic deposits of the Tolmin basin are subdivided into three formations. The lithological characteristics and the main stages of sedimentary evolution are summarized according to Rožič [2009]; for a simplified stratigraphic column, see figure 2b. The Krikov Formation is a 150 to 250 m thick Hettangian to Pliensbachian succession of resedimented limestones that include a distinctive breccia horizon in the lowermost part, approximately at the Triassic-Jurassic boundary. The facies distribution of these gravity-flow deposits indicates that the shallow-water carbonate material was mainly derived from the north, i.e., from the later Julian High, which still acted as a productive carbonate platform during the early Early Jurassic. Crinoidal limestones predominate in the uppermost part of the Krikov Formation and mark the initial stage of tectonically induced drowning in the source area. The overlying Perbla Formation, roughly dated to the Toarcian, is mostly composed of marls and shales with rare intercalations of fine-grained calciturbidites. This formation varies significantly in thickness from 2 to 135 m and thus provides evidence of a considerable basin-floor relief in the late Early Jurassic. The succeeding Tolmin Formation attains a thickness of more than 100 m and is divided into two members. The lower member consists of dark gray, thin-bedded siliceous limestone that alternates with rare chert beds. The upper member consists predominantly of thin-bedded radiolarian chert. Locally, two intervals of carbonate gravity-flow deposits are interstratified within the Tolmin Formation. These two intervals correspond to the lower Bajocian to lower Callovian and to the upper Kimmeridgian to lower Tithonian. During the Middle and Late Jurassic, the carbonate material originated exclusively from the Dinaric Carbonate Platform. The studied succession ends with the upper Tithonian to Neocomian Biancone limestone.

DESCRIPTION OF SECTIONS

Productive radiolarian samples were obtained from three of the six sections described by Rožič [2009]. From south to north, these sections are the Poljubinj, Perbla and Kobla sections (see fig. 2a for their locations and fig. 3 for stratigraphic logs). The studied samples come from the upper member of the Tolmin Formation.

In the Poljubinj section (D48 Coordinates: x=5115550, y=5404500), a 20 m thick succession of radiolarian cherts directly overlies a package of calcareous breccia and bedded calcarenite with abundant ooides. In the lower part, the chert is green, the beds are undulating, and their thickness varies between 2 and 16 cm; shale interlayers constitute 5% of the sequence. Higher in the section, the chert is dark red in color, the beds are even and thinner (2-7 cm), and the proportion of intercalated shale is slightly higher (10%). Some thin beds (2-20 cm) of calcarenite are interstratified within the basal green cherts and within the upper six meters below the Biancone limestone.

At Perbla (D48 Coordinates: x= 5120800, y=5404450), radiolarian cherts overlie siliceous limestone of the lower member of the Tolmin Formation (also see fig. 2b). The upper member of the Tolmin Formation is 57 m thick and predominantly composed of thin (1-10 cm), often laminated chert beds and shales. Shale interlayers generally constitute less than 10% of the rock sequence and are only more abundant in the uppermost few meters of the formation. In places, the chert beds contain some dispersed carbonate at the margins and pure vitreous chert nodules in their middle part. In the first 20 meters, the prevailing color is green, whereas the upper part of the section is mostly violet-red. Calcarenite beds (10 to 50 cm thick) are concentrated near the base and towards the top of the succession, but the middle part is devoid of resedimented limestone.

At Mt. Kobla (D48 Coordinates: x=5121590, y = 5428550), the upper member of the Tolmin Formation, which also conformably overlies the lower member, is 25 m thick and composed of thin-bedded (5-15 cm) black chert. In the upper part, these beds become slightly greenish and finally dark green. In a 3 m thick interval, situated in the lower part, the chert beds are thicker (mostly about 30 cm) and undulate irregularly. The entire succession is free of resedimented limestone, and the proportion of shale does not exceed 5% of the sequence.

BIOSTRATIGRAPHY

Radiolarian dating

More than a hundred radiolarian samples were collected from six well-exposed sections of the Tolmin basin [Rožič, 2009]. Although radiolarians are ubiquitous in thin sections, only eight samples from the three sections (Poljubinj, Perbla and Kobla) yielded determinable radiolarians. All the productive samples are radiolarian cherts and were treated with diluted 9% hydrofluoric acid. The preservation of radiolarians is mostly very poor. Only the samples from Kobla (K3 45.20 and K3 58.70), dominated by small nassellarians, contain some rare pyritized specimens. Such poor preservation along with a very small number of usable samples on the whole is not usual in Mesozoic continental-margin cherts and is probably related to the well-marked deep-burial diagenetic overprint of these rocks [see Rainer *et al.*, 2002]. Various sponge spicules are associated in the lower part of the Poljubinj and Perbla sections but they are never abundant.

The identified radiolarians are illustrated in plates I and II and listed in table I; for the stratigraphic position of the samples, see figure 3. The assemblages were dated with the zonation of Baumgartner *et al.* [1995a] who established 22 Unitary Association Zones (UAZ) for the Middle Jurassic to Early Cretaceous time interval. The ranges of species according to this zonation are presented in table I. New data obtained in the last 15 years show that some species have longer ranges than previously established by Baumgartner *et al.* [1995a]. The ranges have been expanded for the following species on the list in table I: *Striatojaponocapsa synconexa* O'DOGHERTY, GORIČAN and DUMITRICA (it was *Tricolocapsa plicarum* ssp. A in Baumgartner *et al.* [1995c]) now extends up to UAZ 6-7 [Prela *et al.*, 2000; O'Dogherty *et al.*, 2005]; *Zhamoidellum ovum* DUMITRICA and *Zhamoidellum ventricosum* DUMITRICA range down to the UAZ 6-7 [Šmuc and Goričan, 2005]; *Gongylothorax favosus* DUMITRICA and *Hemicryptocapsa carpathica* (DUMITRICA) range up to the Berriasian [Matsuoka, 1998]. Some other species have recently been revised and their taxonomic definitions now differ from those in the catalogue of Baumgartner *et al.* [1995c]; for these species the ranges are not indicated. An example is the three species of *Hexasaturnalis* revised by Dumitrica and Dumitrica-Jud [2005]. Generic names have been updated according to O'Dogherty *et al.* [2009]. Short taxonomic notes are given in the plate captions where necessary. The age assignments are discussed below in stratigraphic order.

UAZ 4 (late Bajocian) and UAZ 5 (latest Bajocian-early Bathonian)

The oldest assemblages occur in the Perbla and Kobla sections. The sample PTR 108.00 (Perbla section) is assigned to UAZ 4 based on the co-occurrence of *Tetraditryma pseudoplena* BAUMGARTNER with *Yaocapsa*? *kisoensis* (YAO) and *Zartus dickinsoni* PESSAGNO and BLOME gr. *Hexasaturnalis suboblongus* (YAO) is also important because it is restricted to the Bajocian [Dumitrica and Dumitrica-Jud, 2005]. The lowest sample from Kobla (K3 45.20) reveals the same UAZ 4 zonal assignment based on the co-occurrence of *Protunuma turbo* MATSUOKA, *Striatojaponocapsa synconexa* O'DOGHERTY, GORIČAN and DUMITRICA, and *Yaocapsa mastoidea* (YAO). The overlying sample, K3 58.70, is constrained to UAZ 5 with the range of *Yaocapsa* aff. *mastoidea* (YAO) (it was *Stichocapsa* sp. E in the catalogue of Baumgartner *et al.* [1995c]).

UAZ 7 (late Bathonian-early Callovian) and UAZ 8 (middle Callovian-early Oxfordian), possibly also UAZ 9 (middle-late Oxfordian) and UAZ 10 (late Oxfordian-early Kimmeridgian)

Radiolarians of UAZ 7 or UAZ 8 were found in the Poljubinj and Perbla sections. The sample POL 30.40 (Poljubinj) contains *Emiluvia orea* BAUMGARTNER and *Lanubus cornutus* (BAUMGARTNER) that first occur in UAZ 8. This sample also contains *Triactoma enzoi* BECCARO, which occurs in zones B to D of Beccaro [2006a], i.e., in the interval that correlates to UAZ 7 and UAZ 8 [for the correlation between the two zonations, see Beccaro, 2006a, p. 43]. The assignment of the sample PTR 114.80 (Perbla section) to UAZ 7-8 is inferred from *Cinguloturris carpatica* DUMITRICA and *Gongylothorax* aff. *favosus* DUMITRICA.

TABLE I. – Occurrence of radiolarian species in the eight productive samples from the three sections studied. The second column gives the zonal ranges of the species according to Baumgartner *et al.* [1995a]; the range of *Triactoma enzoi* is according to Beccaro [2006a]; the arrows indicate that the ranges have been subsequently extended (see the text for references). The zonal assignment of the samples is shown in the bottom row.

TABL. I. – *Distribution des espèces de radiolaires dans les huit échantillons productifs des trois coupes étudiées. La deuxième colonne donne l'extension stratigraphique pour chaque espèce selon les zones de Baumgartner* et al. *[1995a] ; l'extension de* Triactoma enzoi *est donnée d'après Beccaro [2006a] ; les flèches indiquent, que les extensions ont été étendues ultérieurement (voir texte pour les références). La zone déterminée pour chaque échantillon est indiquée dans la dernière ligne.*

sections:		Poljubinj	Perbla					Kobla	
Species **Samples**	**UAZ95**	**POL 30.40**	**PTR 108.00**	**PTR 114.80**	**PTR 119.00**	**PTR 150.40**	**PTR 157.70**	**K3 45.20**	**K3 58.70**
Angulobracchia sicula KITO and DE WEVER	1-6							x	
Archaeodictyomitra apiarium (RÜST)	8-22						x		
Canoptum sp.								x	
Cinguloturris carpatica DUMITRICA gr.	7-11	x		x					
Cinguloturris cylindra KEMKIN and RUDENKO	12-17						x		
Cinguloturris fusiforma HORI					x				
Diacanthocapsa? normalis YAO	3-4								cf.
Diacanthocapsa? sp. A									x
Dicerosaturnalis angustus (BAUMGARTNER)	6-10	x			x				
Emiluvia orea BAUMGARTNER	8-11	x			x	x			
Eoxitus dhimenaensis (BAUMGARTNER) s.l.	3-11							x	x
Eoxitus spinifer (TAKEMURA)									x
Eucyrtidiellum? circumperforatum CHIARI, MARCUCCI and PRELA								x	
Eucyrtidiellum ptyctum (RIEDEL and SANFILIPPO)	5-11				x	x			
Eucyrtidiellum pyramis (AITA)	12-13						x		
Eucyrtidiellum unumaense (YAO)	3-8		x						x
Gongylothorax favosus DUMITRICA	8-10 →				x				
Gongylothorax aff. *favosus* DUMITRICA sensu Baumgartner *et al.* [1995]	7-8			x					
Helvetocapsa matsuokai (SASHIDA)								x	
Hemicryptocapsa buekkensis (KOZUR)					x			x	x
Hemicryptocapsa carpathica (DUMITRICA)	7-11 →				x				
Hemicryptocapsa yaoi (KOZUR)				x				x	x
Hemicryptocapsa sp. A								x	
Hexasaturnalis minor (BAUMGARTNER)				x	x				
Hexasaturnalis nakasekoi DUMITRICA and DUMITRICA-JUD					x				
Hexasaturnalis suboblongus (YAO)			x						
Hiscocapsa? hexagona (HORI)					cf.	cf.			
Hiscocapsa? pseudouterculus (AITA)							x		
Homoeoparonaella argolidensis BAUMGARTNER	4-11	x			x				
Hsuum cf. *mirabundum* PESSAGNO and WHALEN sensu Baumgartner *et al.* [1995]	3-6		x						
Japonocapsa fusiformis (YAO)	3-5		x					x	
Japonocapsa? tegiminis (YAO)								aff.	
Lanubus cornutus (BAUMGARTNER)	8-10	x							
Mirifusus guadalupensis PESSAGNO	5-11	x							
Palinandromeda podbielensis (OZVOLDOVA)	5-9	x							
Pantanellium oligoporum (VINASSA)						x			
Praewilliriedellum convexum (YAO)	1-11		x					x	x
Praewilliriedellum japonicum (YAO)	3-8							x	
Protunuma japonicus MATSUOKA and YAO	7-12				x		x		
Protunuma? lanosus OZVOLDOVA								x	
Protunuma turbo MATSUOKA	4-7							x	
Pseudodictyomitra carpatica (LOZYNIAK)	11-21						x		
Ristola altissima altissima (RÜST)	7-12				x				
Ristola procera (PESSAGNO)	5-9	x		x					
Sella chrafatensis (EL KADIRI)	2-7							x	
Spinosicapsa triacantha (FISCHLI)					x				
Stichomitra? takanoensis AITA gr.	3-7							x	
Striatojaponocapsa synconexa O'DOGHERTY, GORICAN and DUMITRICA	4-5 →							x	x
Tetraditryma pseudoplena BAUMGARTNER	4-11		x						
Theocapsomella medvednicensis (GORICAN)									cf.
Transhsuum brevicostatum (OZVOLDOVA)	3-11				x				
Transhsuum maxwelli (PESSAGNO) gr.	3-10	x		x					
Triactoma blakei (PESSAGNO)	4-11	x			x				
Triactoma enzoi BECCARO	7-8	x							
Triactoma jonesi (PESSAGNO)	2-13		x						
Unuma echinatus ICHIKAWA and YAO	1-6		cf.					cf.	
Unuma latusicostatus (AITA)	2-5							x	
Williriedellum crystallinum DUMITRICA	7-11				x				
Williriedellum formosum (CHIARI, MARCUCCI and PRELA)								x	
Williriedellum spinosum (KOZUR)								x	
Yaocapsa? kisoensis (YAO)	3-4		x						
Yaocapsa mastoidea (YAO)	3-4							x	
Yaocapsa aff. *mastoidea* (YAO) (former *Stichocapsa* sp. E)	5-5								x
Zartus dickinsoni PESSAGNO and BLOME gr.	3-4		x						
Zhamoidellum ovum DUMITRICA	← 9-11	x			x	x	aff.		
Zhamoidellum ventricosum DUMITRICA	← 8-11			x	x				
Age (UAZones 95)		**7-8**	**4**	**7-8**	**8-10**	**8-11**	**12**	**4**	**5**

A note concerning the age of UAZ 7 is necessary here. In the original calibration, this zone comprised the late Bathonian and early Callovian [Baumgartner *et al.*, 1995a]. Later, a diverse radiolarian assemblage of UAZ 7 was described from a sample occurring above early Callovian ammonites and it was concluded that UAZ 7 is mainly Callovian in age [Beccaro, 2006a]. According to these new data and because our sample PTR 114.80 corresponds to UAZ 7-8, we believe this sample is not older than the Callovian.

The sample PTR 119.00 is broadly assigned to UAZ 8 to UAZ 10 based on the first occurrences of *Emiluvia orea* BAUMGARTNER and *Gongylothorax favosus* DUMITRICA and the last occurrence of *Dicerosaturnalis angustus* (BAUMGARTNER).

UAZ 11 (late Kimmeridgian-early Tithonian) and UAZ 12 (early-early late Tithonian)

This interval was dated in the Perbla section. For the sample PTR 150.40, only a very broad assignment of UAZ 8 to UAZ 11 is possible (see the ranges of *Emiluvia orea* BAUMGARTNER and *Eucyrtidiellum ptyctum* (RIEDEL and SANFILIPPO). Considering the stratigraphic position of this sample (see fig. 3), a relatively young age within the determined time span is likely. The topmost sample corresponds to UAZ 12 based on the co-occurrence of *Eucyrtidiellum pyramis* (AITA) and *Cinguloturris cylindra* KEMKIN and RUDENKO with *Protunuma japonicus* MATSUOKA and YAO.

Summary

The base of radiolarian cherts at both distal sections (Perbla and Kobla), where the cherts are in direct contact with the lower member of the Tolmin Formation, is assigned to the upper Bajocian (UAZ 4). Proximally (Poljubinj section), where the limestone turbidites are thicker, the base of the cherts corresponds to the middle Callovian-lower Oxfordian (UAZ 8). The topmost mid-Tithonian (UAZ 12) chert is dated for only one section (Perbla), but the same age is inferred for the other two sections because the base of the Biancone limestone is known to be synchronous throughout the entire Mediterranean.

Nannoplankton dating

Nannoplankton were studied from a marly horizon just below the base of the Biancone limestone at Perbla (sample PTR 158.20). The following taxa were identified (pl. II): *Polycostella beckmannii* THIERSTEIN, *Conusphaera mexicana* TREJO, *Watznaueria* sp., and *Nannoconus* sp. The specimens are relatively well-preserved. Specimens of *Nannoconus* are rare and less well-preserved. Species diversity is low. The assemblage is stratigraphically assignable to the middle-upper Tithonian [Bown, 1998]. According to Bornemann *et al.* [2003], a similar assemblage of calcareous nannoplankton from the Central Atlantic Ocean (DSDP sites 105, 367, 534A) corresponds to the first significant increase in carbonate accumulation in the mid- to late Tithonian interval, which they named the "Nannofossil Calcification Event" (NCE). The second carbonate maximum, which was related to a rise in the absolute abundance of nannofossils, was attributed to the late Berriasian [Bornemann *et al.*, 2003].

STRATIGRAPHIC CORRELATIONS AND DISCUSSION

Regional stratigraphic correlations

An overall correlation between the Tolmin basin and other western Tethyan basins throughout the Toarcian to the Berriasian has already been presented and discussed [Rožič, 2009]. In this paper, we explain in more detail the correlation of the Middle to Upper Jurassic cherts that represent a typical Tethyan radiolarite succession (fig. 3).

The Bajocian increase in the biogenic silica content has been recognized in distal successions of all basins of the western Tethys [see Fig. 5 and Table II for references in Rožič, 2009]. This increase occurs progressively from the lower Bajocian to the lower Bathonian (UAZ 3 to UAZ 5) within individual basins and is, in the Tolmin basin, marked by a distinct boundary between the lower and upper members of the Tolmin Formation. Radiolarian dating at the base of the upper member in the Perbla and Kobla sections (UAZ 4, upper Bajocian) conforms well with the data from the other basins.

The drastic reduction in carbonate content in the western Tethys is now generally interpreted in terms of pronounced sea-water eutrophication because the lithological change coincides with a well-documented positive shift in stable carbon isotopes [Bartolini *et al.*, 1995, 1996, 1999; Jenkyns *et al.*, 2002; Morettini *et al.*, 2002; O'Dogherty *et al.*, 2006]. The rise of the trophic level due to the enhanced continental weathering and associated nutrient supply to oceans during warm and humid climates had a double effect because it not only favored the proliferation of radiolarians in the open sea but also suppressed carbonate production on the adjacent platforms and thus reduced the periplatform carbonate input.

Tectonic subsidence causing the deepening of the basin floor below the CCD was initially proposed to explain the change from carbonate to radiolarite lithologies [Winterer and Bosellini, 1981]. Stratigraphic correlations based on precise radiolarian dating later showed that radiolarites also accumulated at shallower water depths, where other conditions (e.g. high plankton productivity) were favorable [Baumgartner, 1987, 1990]. Although tectonic subsidence is no longer regarded as an ultimate cause of radiolarite deposition, it can still be considered a potential factor that contributed to the depletion of carbonate in deep-sea sediments, especially if the surrounding platform margins also subsided. The Middle Jurassic subsidence, well recognized on a regional scale, is locally best constrained to the north of the study area in the succession of the Bovec basin, where its Bajocian age has been proven by radiolarian dating. In that area, a prominent discontinuity surface separates typical basinal deposits (calcareous turbidites with chert interlayers, dated at their base as UAZ 3 and UAZ 5 in different sections) from the directly underlying Toarcian black shales and the Pliensbachian platform limestones below [Šmuc, 2005; Šmuc and Goričan, 2005].

The Bajocian subsidence was intimately related to the onset of sea-floor spreading in the Alpine Tethys and was concomitant with an intraoceanic subduction in the Neotethys [see Schmid *et al.*, 2008 and the references therein; for reviews of radiolarian biostratigraphic data from ophiolites, see Chiari *et al.*, 2000; Bill *et al.*, 2001;

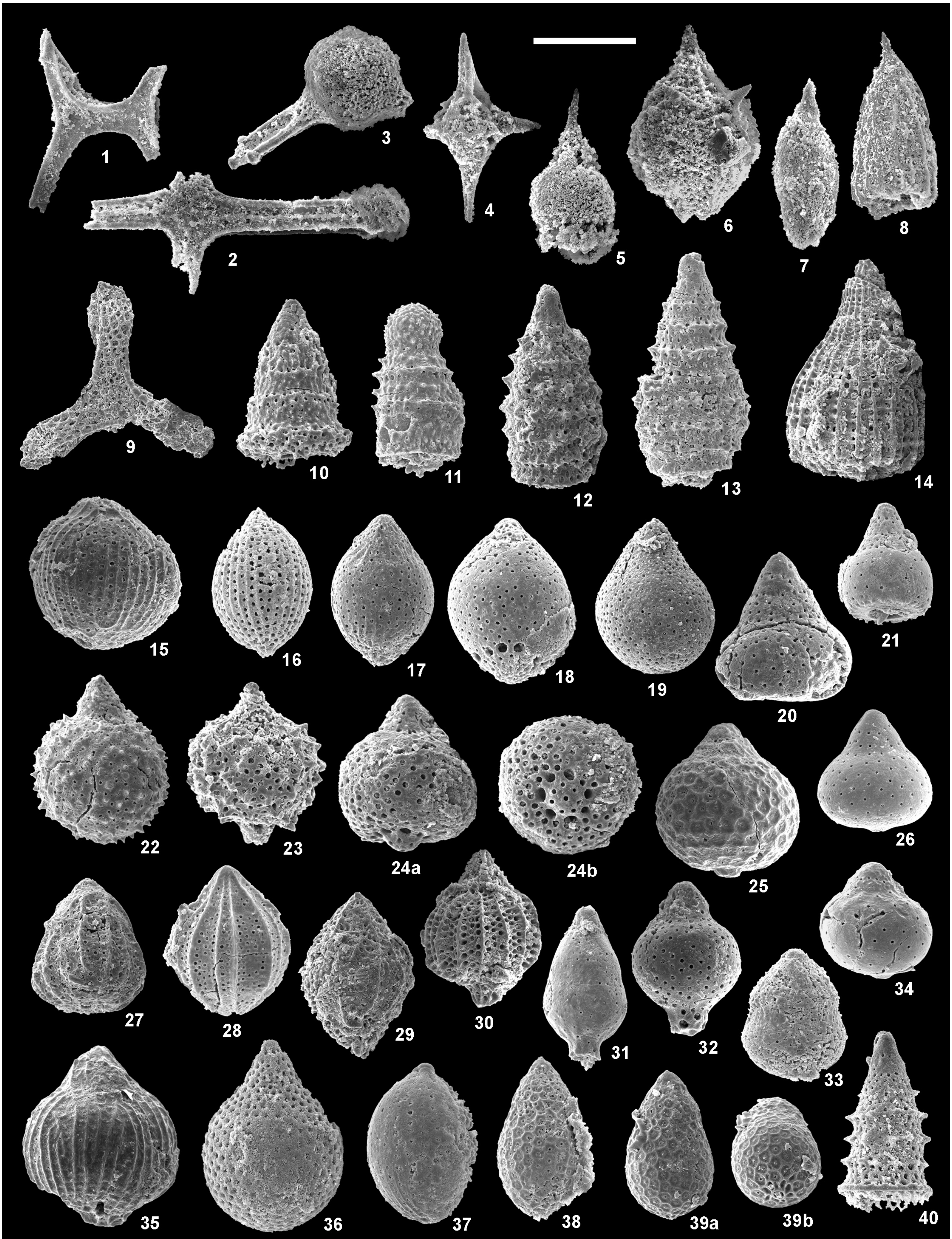
1
2
3
4
5
6
7
8
9
10
11
12
13
14
15
16
17
18
19
20
21
22
23
24a
24b
25
26
27
28
29
30
31
32
33
34
35
36
37
38
39a
39b
40

Baumgartner *et al.*, 2010]. It has been proposed that the opening of a deep-water connection with the eastern Tethys was responsible for substantial modifications in the oceanic circulation that, in turn, had a major long-term impact on climate and surface productivity [Baumgartner, 1987; Bill *et al.*, 2001]. This scenario, based on the redistribution of lithospheric plates, can explain why the deposition of siliceous sediments in the western Tethys persisted for a long time and was not a brief phenomenon restricted to a transient increase in radiolarian productivity.

When compared with the other basins in the southern Alps and in the Apennines, the Tolmin basin contains higher proportions of silica with respect to carbonate throughout the Middle and Upper Jurassic succession [Rožič, 2009]. In contrast, the deep-water basins studied so far in the Dinarides are carbonate-free, except for interbeds of calcareous turbidites [Goričan, 1994; Djerić *et al.*, 2007; Vishnevskaya and Djerić, 2009]. In the Budva basin in southern Montenegro, where shales and cherts occur already in the Aalenian, the Bajocian "event" is only reflected in a progressive increase in the chert/shale ratio [Goričan, 1994]. The elevated content of silica in the Tolmin basin matches well with the paleogeographic position of the basin, close to the northwestern edge of the Neotethys.

The proximal succession of the Tolmin basin (the Poljubinj section) is characterized by resedimented limestones with abundant oolites, and the lowest radiolarian cherts are middle Callovian-early Oxfordian in age (UAZ 8). This succession correlates well with those from other basins adjacent to the Dinaric Carbonate Platform. The upper oolitic turbidites of the Belluno basin were assigned to UAZ 7 [Baumgartner *et al.*, 1995b], but they may range higher, up

PLATE I. – Bajocian to early Bathonian radiolarians. For each illustration, the scanning electron micrograph number and magnification (length of scale bar) are indicated. Rock samples, residues and illustrated specimens are stored at the Ivan Rakovec Institute of Paleontology ZRC SAZU, Ljubljana.
PL. I. – *Radiolaires d'âge bajocien à bathonien inférieur. Pour chaque figure le numéro du cliché MEB et l'agrandissement (longueur de la barre d'échelle) sont précisés. Les échantillons, les résidus et les spécimens illustrés sont conservés dans la collection de l'Institut Ivan Rakovec de Paléontologie ZRC SAZU, Ljubljana.*
Figs. 1-8. – Radiolarians from sample PTR 108.00 (UAZ 4, Perbla section).
Figs. 1-8. – *Radiolaires de l'échantillon PTR 108.00 (UAZ 4, coupe de Perbla).*
1. *Hexasaturnalis suboblongus* (YAO), n°060203, scale bar 100 µm.
2. *Tetraditryma pseudoplena* BAUMGARTNER, n°060206, scale bar 100 µm.
3. *Triactoma jonesi* (PESSAGNO), n°060208, scale bar 133 µm.
4. *Zartus dickinsoni* PESSAGNO and BLOME gr., n°060239, scale bar 100 µm.
5. *Eucyrtidiellum unumaense* (YAO), n°060201, scale bar 80 µm.
6. *Unuma* cf. *echinatus* ICHIKAWA and YAO, n°060229, scale bar 80 µm.
7. *Yaocapsa*? *kisoensis* (YAO), n°060232, scale bar 80 µm.
8. *Hsuum* cf. *mirabundum* PESSAGNO and WHALEN sensu Baumgartner *et al.* [1995c], n°060214, scale bar 100 µm.
Figs. 9-31.– Radiolarians from sample K3 45.20 (UAZ 4, Kobla section).
Figs. 9-31.– *Radiolaires de l'échantillon K3 45.20 (UAZ 4, coupe de Kobla).*
9. *Angulobracchia sicula* KITO and DE WEVER, n°060141, scale bar 200 µm.
10. *Canoptum* sp., n°060131, scale bar 80 µm.
11. *Stichomitra*? *takanoensis* AITA gr., n°060107, scale bar 100 µm.
12, 13. *Eoxitus dhimenaensis* (BAUMGARTNER) s.l., 12: n°060147, 13: n°060113, scale bar 100 µm.
14. *Sella chrafatensis* (EL KADIRI), n°060158, scale bar 133 µm.
15. *Striatojaponocapsa synconexa* O'DOGHERTY, GORIČAN and DUMITRICA, n°060159, scale bar 80 µm.
16. *Helvetocapsa matsuokai* (SASHIDA), n°060108, scale bar 80 µm.
17. *Japonocapsa*? aff. *tegiminis* (YAO), n°060110, scale bar 80 µm. This species differs from the type material [in Yao, 1979] by having some weakly developed longitudinal plicae.
18. *Japonocapsa fusiformis* (YAO), n°060109, scale bar 80 µm.
19. *Praewilliriedellum convexum* (YAO), n°060115, scale bar 100 µm.
20. *Praewilliriedellum japonicum* (YAO), n°060127, scale bar 67 µm.
21. *Eucyrtidiellum*? *circumperforatum* CHIARI, MARCUCCI and PRELA, n°060105, scale bar 80 µm.
22. *Williriedellum spinosum* (KOZUR), n°060157, scale bar 80 µm.
23. *Williriedellum formosum* (CHIARI, MARCUCCI and PRELA), n°060138, scale bar 80 µm.
24a-b. *Hemicryptocapsa* sp. A, n°060156a-b, scale bar 67 µm. In general outline this species is similar to *Hemicryptocapsa marcucciae* (CORTESE) but differs from the latter by its smooth shell with rounded pores.
25. *Hemicryptocapsa yaoi* (KOZUR), n°060161, scale bar 67 µm. *Hemicryptocapsa dierschei* (SUZUKI and GAWLICK) [in Gawlick *et al.*, 2004] is considered a junior synonym of *Hemicryptocapsa yaoi* (KOZUR).
26. *Hemicryptocapsa buekkensis* (KOZUR), n°060128, scale bar 67 µm.
27. *Protunuma*? *lanosus* OŽVOLDOVA, n°060104, scale bar 80 µm.
28. *Protunuma turbo* MATSUOKA, n°060103, scale bar 80 µm.
29. *Unuma* cf. *echinatus* ICHIKAWA and YAO, n°060149, scale bar 100 µm.
30. *Unuma latusicostatus* (AITA), n°060121, scale bar 100 µm.
31. *Yaocapsa mastoidea* (YAO), n°060111, scale bar 80 µm.
Figs. 32-40. – Radiolarians from sample K3 58.70 (UAZ 5, Kobla section).
Figs. 32-40. – *Radiolaires de l'échantillon K3 58.70 (UAZ 5, coupe de Kobla).*
32. *Yaocapsa* aff. *mastoidea* (YAO), n°082213, scale bar 80 µm.
33. *Theocapsomella* cf. *medvednicensis* (GORIČAN), n°082214, scale bar 80 µm.
34. *Hemicryptocapsa buekkensis* (KOZUR), n°082236, scale bar 67 µm.
35. *Striatojaponocapsa synconexa* O'DOGHERTY, GORIČAN and DUMITRICA, n°082210, scale bar 80 µm.
36. *Praewilliriedellum convexum* (YAO), n°082204, scale bar 100 µm.
37. *Diacanthocapsa*? cf. *normalis* YAO, n°082228, scale bar 67 µm.
38, 39a-b. *Diacanthocapsa*? sp. A, 38: n°082221, 39a: n°082208, 39b: n°082209b, scale bar 67 µm. Elongated tricyrtid; cephalis poreless, thorax and abdomen ornamented with polygonal frames, each with a small circular pore in the center; aperture present, sutural pore not observed.
40. *Eoxitus spinifer* (TAKEMURA), n°082217, scale bar 80 µm.

to the UAZ 8, as documented in the sections attributed to the eastern margin of the Trento plateau [Beccaro *et al.*, 2002, 2008]. The oldest cherts above the Middle Jurassic calcareous turbidites of the Budva Zone are also middle Callovian-early Oxfordian (UAZ 8) [Goričan, 1994]. The onset of radiolarite deposition in proximal areas was related to contemporaneous drowning of the adjacent platform [Rožič, 2009] that may have been, as inferred for the Bajocian, induced primarily by eutrophication. The corroborative evidence is the positive carbon isotope shift in the Callovian [Bartolini *et al.*, 1995, 1996, 1999; Jenkyns *et al.*, 2002]. In radiolarian-bearing rocks, this shift was recognized in UAZ 8 [see Bartolini *et al.*, 1995, p. 825].

Siliceous sedimentation then continued in the Late Jurassic due to the establishment of a barrier reef on the platform margin [Turnšek, 1997], which hampered the offshore carbonate transport. At approximately the Early-Late

PLATE II.
Figs. 1-37. – Callovian to Tithonian radiolarians. For each illustration, the scanning electron micrograph number and magnification (length of scale bar) are indicated. Rock samples, residues and illustrated specimens are stored at the Ivan Rakovec Institute of Paleontology ZRC SAZU, Ljubljana.
PL. II.
Figs. 1-37. – *Radiolaires d'âge callovien à bathonien inférieur. Pour chaque figure le numéro du cliché MEB et l'agrandissement (longueur de la barre d'échelle) sont précisés. Les échantillons, les résidus et les spécimens illustrés sont conservés dans la collection de l'Institut Ivan Rakovec de Paléontologie ZRC SAZU, Ljubljana*
Figs. 1-9. – Radiolarians from sample POL 30.40 (UAZ 8, Poljubinj section).
Figs. 1-9. – *Radiolaires de l'échantillon POL 30.40 (UAZ 8, coupe de Poljubinj).*
1. *Triactoma blakei* (PESSAGNO), n°961234, scale bar 200 µm.
2. *Triactoma enzoi* BECCARO, n°961232, scale bar 200 µm.
3. *Lanubus cornutus* (BAUMGARTNER), n°961222, scale bar 200 µm.
4. *Emiluvia orea* BAUMGARTNER, n°961233, scale bar 200 µm.
5. *Palinandromeda podbielensis* (OŽVOLDOVA), n°961223, scale bar 200 µm.
6. *Transhsuum maxwelli* (PESSAGNO), n°961231, scale bar 133 µm.
7. *Cinguloturris carpatica* DUMITRICA, n°961228, scale bar 133 µm.
8. *Mirifusus guadalupensis* PESSAGNO, n°961231, scale bar 200 µm.
9. *Ristola procera* (PESSAGNO), n°961606, scale bar 200 µm.
Figs. 10-13. – Radiolarians from sample PTR 114.80 (UAZ 7-8, Perbla section).
Figs. 10-13. – *Radiolaires de l'échantillon PTR 114.80 (UAZ 7-8, coupe de Perbla).*
10. *Hexasaturnalis minor* (BAUMGARTNER), n°090102, scale bar 133 µm.
11a-b. *Gongylothorax* aff. *favosus* DUMITRICA sensu Baumgartner *et al.* [1995c], 11a: n°090125, 11b: n°090126, scale bar 80 µm.
12. *Hemicryptocapsa yaoi* (KOZUR), n°090105, scale bar 80 µm. See remarks under pl. I, fig. 25.
13. *Zhamoidellum ventricosum* DUMITRICA, n°090113, scale bar 100 µm.
Figs. 14-26 – Radiolarians from sample PTR 119.00 (UAZ 8-10, Perbla section).
Figs. 14-26. – *Radiolaires de l'échantillon PTR 119.00 (UAZ 8-10, coupe de Perbla).*
14. *Cinguloturris fusiforma* HORI, n°060334, scale bar 100 µm.
15. *Ristola altissima altissima* (RÜST), n°060338, scale bar 200 µm.
16. *Homoeoparonaella argolidensis* BAUMGARTNER, n°060424, scale bar 200 µm.
17. *Dicerosaturnalis angustus* (BAUMGARTNER), n°060420, scale bar 133 µm.
18. *Hexasaturnalis minor* (BAUMGARTNER), n°060421, scale bar 133 µm.
19. *Hexasaturnalis nakasekoi* DUMITRICA and DUMITRICA-JUD, n°060422, scale bar 133 µm.
20. *Hemicryptocapsa carpathica* (DUMITRICA), n°060304, scale bar 100 µm.
21. *Eucyrtidiellum ptyctum* (RIEDEL and SANFILIPPO), n°060316, scale bar 80 µm.
22. *Williriedellum crystallinum* DUMITRICA, n°060306, scale bar 100 µm.
23. *Gongylothorax favosus* DUMITRICA, n°060311, scale bar 80 µm.
24. *Spinosicapsa triacantha* (FISCHLI), n°060408, scale bar 133 µm.
25. *Transhsuum brevicostatum* (OŽVOLDOVA), n°060415, scale bar 133 µm.
26. *Hiscocapsa*? cf. *hexagona* (HORI), n°060329, scale bar 80 µm.
Figs. 27-30. - Radiolarians from sample PTR 150.40 (UAZ 11 or slightly older, Perbla section).
Figs. 27-30. - *Radiolaires de l'échantillon PTR 150.40 (UAZ 11 ou un peu plus ancien, coupe de Perbla).*
27. *Emiluvia orea* BAUMGARTNER, n°090118, scale bar 133 µm.
28. *Pantanellium oligoporum* (VINASSA), n°090201, scale bar 133 µm.
29. *Hiscocapsa*? cf. *hexagona* (HORI), n°090219, scale bar 80 µm.
30. *Zhamoidellum ovum* DUMITRICA, n°090202, scale bar 100 µm.
Figs. 31-37. – Radiolarians from sample PTR 157.70 (UAZ 12, Perbla section).
Figs. 31-37. – *Radiolaires de l'échantillon PTR 157.70 (UAZ 12, coupe de Perbla).*
31. *Pseudodictyomitra carpatica* (LOZYNIAK), n°090325, scale bar 100 µm.
32. *Cinguloturris cylindra* KEMKIN and RUDENKO, n°090320, scale bar 100 µm.
33. *Archaeodictyomitra apiarium* (RÜST), n°090315, scale bar 100 µm.
34. *Protunuma japonicus* MATSUOKA and YAO, n°090304, scale bar 100 µm.
35. *Hiscocapsa*? *pseudouterculus* (AITA), n°090303, scale bar 80 µm.
36. *Eucyrtidiellum pyramis* (AITA), n°090319, scale bar 80 µm.
37. *Zhamoidellum* aff. *ovum* DUMITRICA, n°090321, scale bar 100 µm. This species differs from the type material by its shorter cephalothorax and large sutural pore.
Figs. 38-43. – Tithonian calcareous nannofossils from sample PTR 158.20 (Perbla section), XPL images. The illustrated material is stored at the Department of Geology, Faculty of Natural Sciences and Engineering, University of Ljubljana.
Figs. 38-43. – *Nannofossiles calcaires du Tithonien de l'échantillon PTR 158.20 (coupe de Perbla), images XPL. Le matériel illustré est conservé dans la collection du Département de Géologie, Faculté des Sciences Naturelles et de Technologie, Université de Ljubljana.*
38, 39. *Conusphaera mexicana* TREJO, scale bar 5 µm.
40, 41. *Polycostella beckmannii* THIERSTEIN, scale bar 5 µm.
42. *Nannoconus* sp., scale bar 5 µm.
43. *Watznaueria* sp., scale bar 5 µm.

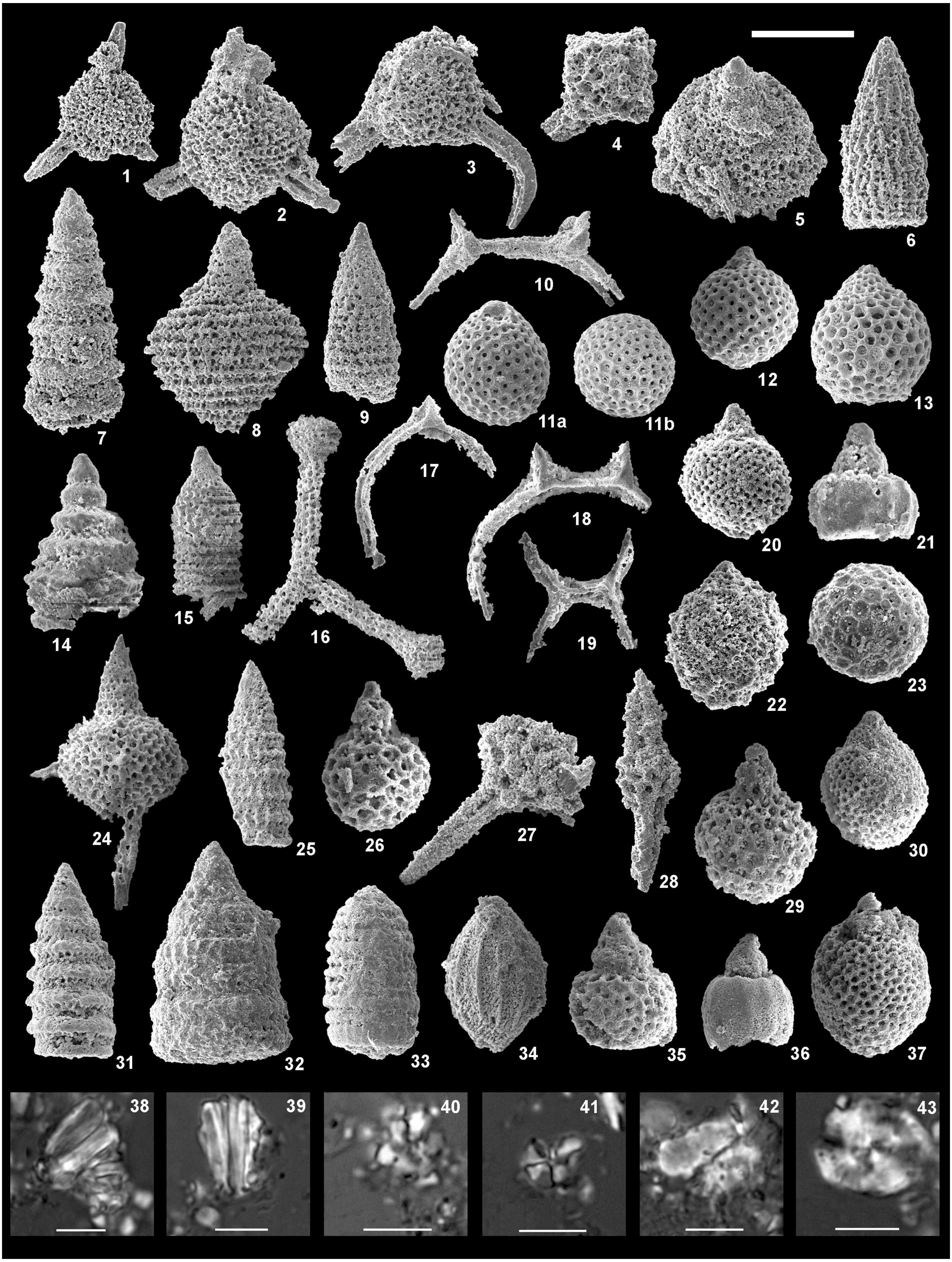
1
2
3
4
5
6
7
8
9
10
11a
11b
12
13
14
15
16
17
18
19
20
21
22
23
24
25
26
27
28
29
30
31
32
33
34
35
36
37
38
39
40
41
42
43

Tithonian boundary, silica-rich sediments were replaced by pelagic limestones simultaneously in all western Tethyan basins [Baumgartner, 1984, 1987; De Wever *et al.*, 1994 etc.]. In the Tolmin basin the contact between the two lithologies is well pronounced. This abrupt facies change agrees well with data from other basins in the Dinarides [e.g., the Budva basin, Goričan, 1994], but is in significant contrast with the gradual transition between the Rosso ad Aptici and the Maiolica Limestone in the basinal successions of the southern Alps [Baumgartner, 1984, 1987; Chiari *et al.*, 2007].

Intrabasinal distribution of radiolarian cherts

Vertical and lateral facies changes occur within the Jurassic radiolarite successions of all Tethyan basins. The most apparent is the change in color from variegated or green below to red-colored radiolarites above [Baumgartner, 1984, 1987 etc.]. Although the general sequence of colors is the same in all basins, it is also well known that the color change from green to red radiolarites is diachronous regionally [Baumgartner, 1984] and even locally within one basin [Goričan, 1994]. The same diachronism, although less well dated, seems to occur in the Tolmin basin (fig. 3) where the Upper Jurassic cherts of the Poljubinj and Perbla sections are red, and the probably coeval cherts at Kobla are green. It has been suggested that the color of cherts can be regarded as an indicator of local paleobathymetry [Goričan, 1994]. Black to green cherts accumulated in topographically higher areas within or close to the oxygen minimum zone, whereas red cherts were deposited in greater depths below the oxygen minimum zone. The prevalence of dark cherts throughout the basin in the Middle Jurassic can be explained by a wider oxygen minimum layer that expanded down to the basin sill, and may have resulted from the higher plankton productivity during this time interval.

It is also interesting to compare the thickness of radiolarite successions in time slices (fig. 3). The overall comparison of sediment thickness from the Toarcian to the Tithonian [also see Rožič, 2009] suggests that, among the three sections studied in this paper, the Perbla section was the closest to the depocenter. However, the Perbla section is less than 8 m thick for the late Bajocian to Callovian interval between the samples PTR 108.00 (UAZ 4) and PTR 114.80 (UAZ 7-8), whereas the Kobla section has a 13.5 m thick succession for a much shorter Bajocian to early Bathonian time interval between the samples K3 45.20 (UAZ 4) and K3 58.70 (UAZ 5). It thus seems reasonable to conclude that a great part of the sedimentary succession originally deposited at Perbla was later removed. No erosional truncation is evident in the outcrop and we can only guess that the bedding plane of the silicified calcareous turbidite just below the sample PTR 114.80 would be a suitable candidate for a hidden discontinuity surface [sensu Clari *et al.*, 1995]. We also note that at the Poljubinj section the correlative contact between the calcareous turbidites and the radiolarian cherts is very abrupt and may correspond to a stratigraphic gap. It is tempting to assume that tectonic activity in the late Bathonian or Callovian (prior to the documented UAZ 7-8 at Perbla and UAZ 8 at Poljubinj) caused the down-slope sliding of semi-consolidated sediment, but the present data are insufficient to demonstrate the wider lateral reproducibility of this event or to detect a distal equivalent (possibly a slumped interval) of the presumed mass movement. Within the limits of biostratigraphic resolution, this event can be considered contemporaneous with the Middle-Late Callovian synsedimentary block-faulting documented in the Rosso Ammonitico Veronese of the Trento plateau in the southern Alps [Martire, 1996]. Whatever the trigger, it is clear that substantial redeposition of pelagic sediments did occur within the basin because the vertical changes in thickness can have opposite trends in different sections. In the Perbla section, the Upper Jurassic interval is approximately four times thicker than the Middle Jurassic interval, whereas the relationship in the Kobla section is the inverse (see fig. 3 for the contrasting thickness of the two successive intervals at these two sections). This observation means that the variations in thickness were mainly determined by the instability of depositional slopes and not simply by variations in the productivity of siliceous plankton, which would have produced parallel trends in different parts of the basin. Similar, although less striking, spatiotemporal variations in thickness were observed in the Lombardian basin [Chiari *et al.*, 2007]. The predominant control of local paleotopography on the accumulation rates of biosiliceous sediments can probably be generalized to all narrow, fault-bounded rift basins.

CONCLUSIONS

The radiolarian cherts of the Tolmin basin range in age from the late Bajocian to the early Tithonian. This time span agrees well with the time span established in other basinal successions of the western Tethys.

On a regional scale, the Bajocian change from carbonate- to chert-dominated lithologies represents a fundamental change in the depositional history of western Tethyan continental-margin basins. This event occurred concomitantly with the reorganization of plate boundaries (the opening of the Alpine Tethys and the intraoceanic subduction in the Meliata-Maliac-Vardar Ocean), regional subsidence, and an increase in surface productivity.

On a local (intrabasinal) scale, it is worth emphasizing the contrasting variations in the thickness of radiolarian cherts in different sections. This distributional pattern was primarily determined by the redeposition of siliceous sediments. Thickness variations mainly reflect the complex topography of the basin floor and potentially unravel synsedimentary tectonic pulses, but short-term productivity fluctuations may be completely masked.

Acknowledgements. – Funding for this work was provided by the research programs P1-0008 and P1-0195 of the Slovenian Research Agency. We thank Marco Chiari, Atsushi Takemura and Catherine Crônier for their thorough reviews.

References

BARTOLINI A., BAUMGARTNER P.O. & MATTIOLI E. (1995). – Middle and Late Jurassic radiolarian biostratigraphy of the Colle Bertone and Terminilletto sections (Umbria-Marche-Sabina Apennines, Central Italy): an integrated stratigraphical approach. *In*: P.O. BAUMGARTNER, L. O'DOGHERTY, Š. GORIČAN, E. URQUHART, A. PILLEVUIT & P. DE WEVER, Eds., Middle Jurassic to Lower Cretaceous Radiolaria of Tethys: Occurrences, systematics, biochronology. – *Mémoires de Géologie (Lausanne)*, **23**, 817-832.

BARTOLINI A., BAUMGARTNER P.O. & HUNZIKER J.C. (1996). – Middle and Late Jurassic carbon stable-isotope stratigraphy and radiolarite sedimentation of the Umbria-Marche Basin (Central Italy). – *Eclogae geol. Helv.*, **89**, 831-879.

BARTOLINI A., BAUMGARTNER P.O. & GUEX J. (1999). – Middle and Late Jurassic radiolarian palaeoecology versus carbon-isotope stratigraphy. – *Palaeogeogr., Palaeoclimatol., Palaeoecol.*, **145**, 43-60.

BAUMGARTNER P.O. (1984). – A Middle Jurassic – Early Cretaceous low-latitude radiolarian zonation based on unitary associations and age of Tethyan radiolarites. – *Eclogae geol. Helv.*, **77**, 729-837.

BAUMGARTNER P.O. (1987). – Age and genesis of Tethyan Jurassic radiolarites. – *Eclogae geol. Helv.*, **80**, 831-879.

BAUMGARTNER P.O. (1990). – Genesis of Jurassic Tethyan radiolarites – The example of Monte Nerone (Umbria-Marche Apennines). *In*: G. PALLINI, F. CECCA, S. CRESTA & M SANTANTONIO, Eds., *Atti del secondo convegno internazionale Fossili, Evoluzione, Ambiente*, Pergola 1987, 19-32.

BAUMGARTNER P.O., DE WEVER P. & KOCHER R. (1980). – Correlation of Tethyan Late Jurassic-Early Cretaceous radiolarian events. – *Cahier de Micropaléontologie*, **2**, 23-86.

BAUMGARTNER P.O., BARTOLINI A., CARTER E.S., CONTI M., CORTESE G., DANELIAN T., DE WEVER P., DUMITRICA P., DUMITRICA-JUD R., GORIČAN Š., GUEX J., HULL D.M., KITO N., MARCUCCI M., MATSUOKA A., MURCHEY B., O'DOGHERTY L., SAVARY J., VISHNEVSKAYA V., WIDZ D. & YAO A. (1995a). – Middle Jurassic to Early Cretaceous radiolarian biochronology of Tethys based on Unitary Associations. *In*: P.O. BAUMGARTNER, L. O'DOGHERTY, Š. GORIČAN, E. URQUHART, A. PILLEVUIT & P. DE WEVER, Eds., Middle Jurassic to Lower Cretaceous Radiolaria of Tethys: Occurrences, systematics, biochronology. – *Mémoires de Géologie (Lausanne)*, **23**, 1013-1038.

BAUMGARTNER P.O., MARTIRE L., GORIČAN Š., O'DOGHERTY L., ERBA E. & PILLEVUIT A. (1995b). – New Middle and Upper Jurassic radiolarian assemblages co-occurring with ammonites and nannofossils from the southern Alps (northern Italy *In*: P.O. BAUMGARTNER, L. O'DOGHERTY, Š. GORIČAN, E. URQUHART, A. PILLEVUIT & P. DE WEVER, Eds., Middle Jurassic to Lower Cretaceous Radiolaria of Tethys: Occurrences, systematics, biochronology. – *Mémoires de Géologie (Lausanne)*, **23**, **23**, 737-749.

BAUMGARTNER P.O., O'DOGHERTY L., GORIČAN Š., DUMITRICA-JUD R., DUMITRICA P., PILLEVUIT A., URQUHART E., MATSUOKA A., DANELIAN T., BARTOLINI A., CARTER E.S., DE WEVER P., KITO N., MARCUCCI M. & STEIGER T. (1995c). – Radiolarian catalogue and systematics of Middle Jurassic to Early Cretaceous Tethyan genera and species. *In*: P.O. BAUMGARTNER, L. O'DOGHERTY, Š. GORIČAN, E. URQUHART, A. PILLEVUIT & P. DE WEVER, Eds., Middle Jurassic to Lower Cretaceous Radiolaria of Tethys: Occurrences, systematics, biochronology. – *Mémoires de Géologie (Lausanne)*, **23**, **23**, 37-685.

BAUMGARTNER P.O., GORIČAN Š. & CHIARI M. (2010). – Ophiolites in the Dinarides and Hellenides: the contribution of radiolarian biochronology to the understanding of their formation and emplacement. *In*: Abstracts Volume, *XIX Congress of the Carpathian-Balkan Geological Association,* Thessaloniki, 40-41.

BECCARO P. (2006a). – Radiolarian biostratigraphy of Middle-Upper Jurassic pelagic siliceous successions of western Sicily and the southern Alps (Italy). – *Mémoires de Géologie (Lausanne)*, **45**, 1-87, pls. 1-12.

BECCARO P. (2006b). – Radiolarian correlation of Jurassic siliceous successions of the Rosso Ammonitico Formation in the southern Alps and western Sicily (Italy). – *Eclogae geol. Helv.*, **99**, Suppl. 1, S21-S33.

BECCARO P., BAUMGARTNER P.O. & MARTIRE L. (2002). – Radiolarian biostratigraphy of the Fonzaso Formation, Middle-Upper Jurassic, southern Alps, Italy. – *Micropaleontology*, **48**, suppl. 1, 43-60.

BECCARO P., DISERENS M.-O., GORIČAN Š. & MARTIRE L. (2008). – Callovian radiolarians from the lowermost Calcare Selcifero di Fonzaso at Ponte Serra (Trento Plateau, Southern Alps, Italy). – *Rivista Italiana di Paleontologia e Stratigrafia*, **114**, 489-504.

BERNOULLI D., BERTOTTI G. & FROITZHEIM N. (1990). – Mesozoic faults and associated sediments in the Austroalpine-South Alpine continental margin. – *Mem. Soc. Geol. Ital.*, **45**, 25-38.

BERRA F., GALLI, M.T., REGHELLIN F., TORRICELLI S. & FANTONI R. (2009). – Stratigraphic evolution of theTriassic-Jurassic succession in the western southern Alps (Italy): the record of the two-stage rifting on the distal passive margin of Adria. – *Basin Res.*, **21**, 335-353.

BERTOTTI G., PICOTTI V., BERNOULLI D. & CASTELLARIN A. (1993). – From rifting to drifting: tectonic evolution of the South-Alpine upper crust from the Triassic to the Early Cretaceous. – *Sediment. Geol.,* **86**, 53-76.

BILL M., O'DOGHERTY L., GUEX J., BAUMGARTNER P. O. & MASSON H. (2001). – Radiolarite ages in Alpine-Mediterranean ophiolites: Constraints on the oceanic spreading and the Tethys-Atlantic connection. – *Geol. Soc. Amer. Bull.*, **113**, 129–143.

BORNEMANN A., ASCHWER U. & MUTTERLOSE J. (2003). – The impact of calcareous nannofossils on the pelagic carbonate accumulation across the Jurassic-Cretaceous boundary. – *Palaeogeogr., Palaeoclimatol., Palaeoecol.*, **199**, 187-228.

BOWN P. (1998). – Calcareous nannofossil biostratigraphy. – Kluwer Acad. Publ., 314 p.

BUSER S. (1986). – Osnovna geološka karta SFRJ 1: 100.000. Tolmač listov Tolmin in Videm (Udine). – Zvezni geološki zavod, Beograd, 103 p.

BUSER S. (1987). – Osnovna geološka karta SFRJ 1: 100 000, list Tolmin in Videm. – Zvezni geološki zavod, Beograd.

BUSER S. (1996). – Geology of western Slovenia and its paleogeographic evolution. *In*: K. DROBNE, Š. GORIČAN & B. KOTNIK, Eds., The role of impact processes in the geological and biological evolution of planet Earth. – *International workshop*, ZRC SAZU, Ljubljana, 111-123.

CHIARI M., MARCUCCI M. & PRINCIPI G. (2000). – The age of the radiolarian cherts associated with the ophiolites in the Apennines (Italy) and Corsica (France): a revision. – *Ofioliti*, **25**, 141-146.

CHIARI M., COBIANCHI M. & PICOTTI V. (2007). – Integrated stratigraphy (radiolarians and calcareous nannofossils) of the Middle to Upper Jurassic Alpine radiolarites (Lombardian basin, Italy): Constraints to their genetic interpretation. – *Palaeogeogr., Palaeoclimatol., Palaeoecol.*, **249**, 233-270.

CLARI P.A., DELA PIERRE F. & MARTIRE L (1995). – Discontinuities in carbonate successions: identification, interpretation and classification of some Italian examples. – *Sediment. Geol.*, **100**, 97-121.

COUSIN M. (1970). – Esquise géologique des confins italo-yougoslaves: leur place dans les Dinarides et les Alpes méridionales. – *Bull. Soc. géol. Fr.*, (7), **XII**, 1034-1047.

COUSIN M. (1973). – Le sillon slovène: les formations triasiques, jurassiques et néocomiennes au Nord-Est de Tolmin (Slovénie occidentale, Alpes méridionales) et leurs affinités dinariques. – *Bull. Soc. géol. Fr.*, (7), **XV**, 326-339.

COUSIN M. (1981). – Les rapports Alpes-Dinarides. Les confins de l'Italie et de la Yougoslavie. – *Soc. géol. Nord Publ.*, **5**, Vol. I: 521 p., Vol. II Annexe: 521 p.

DANELIAN T., DE WEVER P. & VRIELYNCK B. (1986). – Datations nouvelles fondées sur les faunes de radiolaires de la série jurassique des Schistes à Posidonies (Zone Ionienne, Epire, Grèce). – *Rev. Paléobiol.*, **5**, 37-41.

DANELIAN T. & BAUDIN F. (1990). – Découverte d'un horizon carbonaté, riche en matière organique au sommet des radiolarites d'Epire (zone ionienne, Grèce): le Membre de Paliambela. – *C. R. Acad. Sciences,* Paris, **311**, 421-428.

DANELIAN T., DE WEVER P. & AZÉMA J. (1997). – Palaeoceanographic significance of new and revised palaeontological datings for the onset of Vigla Limestone sedimentation in the Ionian zone of Greece. – *Geol. Mag.*, **134**, 869-872.

De Wever P. & Miconnet P. (1985). – Datations directes des radiolarites du bassin du Lagonero (Lucanie, Italie méridionale). Implications et conséquences. – *Rev. españ. Micropal.*, **17**, 373-402.

De Wever P. & Cordey F. (1986). – Datation par les radiolaires de la formation des radiolarites s.s. de la Série du Pinde-Olonos (Grèce): Bajocien (?)-Tithonique. – *Mar. Micropal.*, **11**, 113-127.

De Wever P., Azéma J. & Fourcade E. (1994). – Radiolaires et radiolarites: production primaire, diagenèse et paléogéographie (Radiolarians and radiolarites: primary production, diagenesis and paleogeography). – *Bull. Centres Rech. Explor.-Prod. Elf Aquitaine*, **18**, 315-379.

Djerić N., Gerzina N. & Schmid S.M. (2007). – Age of the Jurassic radiolarian chert formation from the Zlatar mountain (SW Serbia). – *Ofioliti*, **32**, 101-108.

Doglioni C. & Bosellini A. (1987). – Eoalpine and mesoalpine tectonics in the southern Alps. – *Geol. Rundsch.,* **76**, 735-754.

Doglioni C. & Siorpaes C. (1990). – Polyphase deformation in the Col Bechei area (Dolomites-northern Italy). – *Eclogae geol. Helv.*, **83**, 701-710.

Dumitrica P. & Dumitrica-Jud R. (2005). – *Hexasaturnalis nakasekoi* nov. sp., a Jurassic saturnalid radiolarian species frequently confounded with *Hexasaturnalis suboblongus* (Yao). – *Rev. Micropal.*, **48**, 159-168.

Gawlick H.-J., Schlagintweit F., Ebli O. & Suzuki H. (2004). – Die Plassen-Formation (Kimmeridgium) des Krahstein (Steirisches Salzkammergut, Österreich) und ihre Unterlagerung: neue Daten zur Fazies, Biostratigraphie und Sedimentologie. – *Zentralbl. Geol. Paläontol.*, Teil 1, **2003** (3/4), 295-334.

Goričan Š. (1994). – Jurassic and Cretaceous radiolarian biostratigraphy and sedimentary evolution of the Budva Zone (Dinarides, Montenegro). – *Mémoires de Géologie (Lausanne)*, **18**, 1-177.

Goričan Š, Rožič B. & Pavšič J. (2006). – Datacije jurskih radiolarijskih rožencev Tolminskega pokrova. *In*: Zbornik povzetkov*, Slovenski geološki kongres*, Idrija, 46-47.

Jenkyns H.G., Jones C.E., Gröcke D.R., Hesselbo S.P. & Parkinson D.N. (2002). – Chemostratigraphy of the Jurassic System: applications, limitations and implications for palaeoceanography. – *J. Geol. Soc., London*, **159**, 351-378.

Kocher R.N. (1981). – Biochronostratigraphische Untersuchungen oberjurassischer radiolarienführender Gesteine, insbesondere der Südalpen. – *Mitteilungen aus dem geologischen Institut der Eidgenossischen Technischen Hochschule und der Universität Zürich*, Neue Folge, **234**, 184 p.

Kukoč D., Goričan Š & Košir A. (2012). – Lower Cretaceous carbonate gravity-flow deposits from the Bohinj area (NW Slovenia): evidence of a lost carbonate platform in the Internal Dinarides. In: T. Danelian & Š. Goričan, Eds., Radiolarian biochronology as key to tectono-stratigraphic reconstructions. – *Bull. Soc. géol. Fr.*, **183**, 4, 383-392.

Martire L. (1996). – Stratigraphy, facies and synsedimentary tectonics in the Jurassic Rosso Ammonitico Veronese (Altopiano di Asiago, NE Italy). – *Facies*, **35**, 209-236.

Matsuoka A. (1998). – Faunal composition of earliest Cretaceous (Berriasian) radiolaria from the Mariana Trench in the western Pacific. – *News of Osaka Micropaleontologists*, Special Volume, **11**, 165-187.

Morettini E., Santantonio M., Bartolini A., Cecca F., Baumgartner P.O. & Hunziker J.C. (2002). – Carbon isotope stratigraphy and carbonate production during the Early-Middle Jurassic: examples from the Umbria-Marche-Sabina Apennines (central Italy). – *Palaeogeogr., Palaeoclimatol., Palaeoecol.*, **184**, 251-273.

O'Dogherty L., Bill M., Goričan Š., Dumitrica P. & Masson H. (2005). – Bathonian radiolarians from an ophiolitic mélange of the Alpine Tethys (Gets nappe, Swiss-French Alps). – *Micropaleontology*, **51**, 425-485.

O'Dogherty L., Sandoval J., Bartolini A., Bruchez S., Bill M. & Guex J. (2006). – Carbon-isotope stratigraphy and ammonite faunal turnover for the Middle Jurassic in the southern Iberian paleomargin. – *Palaeogeogr., Palaeoclimatol., Palaeoecol.*, **239**, 311-333.

O'Dogherty L., Carter E.S., Dumitrica P., Goričan Š., De Wever P., Bandini A.N., Baumgartner P.O. & Matsuoka A. (2009). – Catalogue of Mesozoic radiolarian genera. Part 2: Jurassic-Cretaceous. – *Geodiversitas*, **31**, 271-356.

Placer L. (1999). – Contribution to the macrotectonic subdivision of the border region between southern Alps and External Dinarides. – *Geologija*, **41** (1998), 223-255.

Prela M., Chiari M. & Marcucci M. (2000). – Jurassic radiolarian biostratigraphy of the sedimentary cover of ophiolites in the Mirdita area, Albania: new data. – *Ofioliti*, **25**, 55-62.

Rainer T., Herlec U., Rantitsch G., Sachsenhofer R.F. & Vrabec M. (2002). – Organic matter maturation vs clay mineralogy: A comparison for Carboniferous to Eocene sediments from the Alpine-Dinaride junction (Slovenia, Austria). – *Geologija*, **45**, 513-518.

Rainer T., Sachsenhofer R.F., Rantitsch G., Herlec U. & Vrabec M. (2009). – Organic maturity trends across the Variscan discordance in the Alpine-Dinaric Transition Zone (Slovenia, Austria, Italy): Variscan versus Alpidic thermal overprint. – *Austrian J. Earth Sci.*, **102**, 120-133.

Rožič B. (2006). – Sedimentology, stratigraphy and geochemistry of Jurassic rocks in the western part of the Slovenian basin. – Ph.D. Thesis, 148 p., University of Ljubljana. – Central Technological Library at the University of Ljubljana (CTK).

Rožič B. (2009). – Perbla and Tolmin formations: revised Toarcian to Tithonian stratigraphy of the Tolmin basin (NW Slovenia) and regional correlations. – *Bull. Soc. géol. Fr.,* **180**, 411-430.

Rožič B. & Popit T. (2006). – Resedimented limestones in Middle and Upper Jurassic succession of the Slovenian basin. – *Geologija*, **49**, 219-234.

Sarti M., Bosellini A. & Winterer E.L. (1992). – Basin geometry and architecture of a Tethyan passive margin, southern Alps, Italy. *In*: J.S. Watkins, F. Zhiqiang and K.J. McMillen, Eds., Geology and geophysics of continental margins. – *AAPG Mem.*, **53**, 241-258.

Schettino A. & Turco E. (2011). – Tectonic history of the western Tethys since the Late Triassic. – *Geol. Soc. Amer. Bull.*, **123**, 89-105.

Schmid M.S., Bernoulli D., Fügenschuh B., Matenco L., Schefer S., Schuster R., Tischler M. & Ustaszewski K. (2008). – The Alpine-Carpathian-Dinaridic orogenic system: correlation and evolution of tectonic units. – *Swiss J. Geosci.*, **101**, 139-183.

Šmuc A. (2005). – Jurassic and Cretaceous stratigraphy and sedimentary evolution of the Julian Alps, NW Slovenia. – Založba ZRC/ZRC Publishing, Ljubljana, 98 p.

Šmuc A. & Goričan Š. (2005). – Jurassic sedimentary evolution of a carbonate platform into a deep-water basin, Mt. Mangart (Slovenian-Italian border). – *Riv. Ital. Paleont. Stratigr.*, **111**, 45-70.

Turnšek D. (1997). – Mezosoic corals of Slovenia. – ZRC/ZRC Publishing, Ljubljana, 512 p.

Vishnevskaya V.S. & Djerić N. (2009). – Mesozoic radiolaria of Bosnia and Serbia: new data. – *Paleont. J.*, **43**, 1513-1568.

Winterer E.L. & Bosellini A. (1981). – Subsidence and sedimentation on Jurassic passive continental margin, southern Alps, Italy. – *AAPG Bull.*, **65**, 394-421.

Yao A. (1979). – Radiolarian fauna from the Mino belt in the northern part of the Inuyama area, Central Japan. Part II: Nassellaria 1. – *J. Geosci.,* Osaka City University, **22**, 21-72.